Ultrasonic pulses in a glass forming salt melt near T g . A time and space resolved study using interferometry

G. Arachovitis, B. Balschun, M. Soltwisch, and D. Quitmann

Citation: The Journal of Chemical Physics **103**, 9574 (1995); doi: 10.1063/1.469972
View online: http://dx.doi.org/10.1063/1.469972
View Table of Contents: http://scitation.aip.org/content/aip/journal/jcp/103/22?ver=pdfcov
Published by the AIP Publishing

Ultrasonic pulses in a glass forming salt melt near T_g. A time and space resolved study using interferometry

G. Arachovitis, B. Balschun, M. Soltwisch, and D. Quitmann
Freie Universität Berlin, Inst. f. Experimentalphysik, Arnimallee 14, D 14195 Berlin, Germany

(Received 30 December 1994; accepted 5 September 1995)

An optoacoustic experiment was set up to study generation, propagation, and damping of broadband acoustic pulses in the MHz region. The sound pulse front is detected interferometrically. The analysis is based on linear hydrodynamic theory and comprises diffraction of the sound pulse. To introduce relaxational effects, it was extended by splitting the specific heat into a ''fast'' and a ''slow'' part. Thus, a good description of the observed pulse shapes and speeds could be obtained. Results for the glass forming 1-methyl-3-ethyl-imidazoliumchloride-$AlCl_3$ mixture at three concentrations and for temperatures between -80 °C and $+20$ °C are reported. © *1995 American Institute of Physics.*

I. INTRODUCTION

The dramatic slowing down of relaxation in the liquid-to-glass transition induces a considerable dependence of the elastic moduli on temperature and frequency. For an understanding of the glass transition, it is important to observe these dependencies over the full temperature range, and over a frequency range as wide as possible. Optical techniques of observation have the advantages of being fast, nonintrusive and applicable for arbitrary temperatures, i.e., arbitrary viscosities.

In the present work, we combined the technique of optoacoustic (for excitation of sound pulses) with a Mach–Zehnder interferometer (for detection of the sound pulses). For excitation, a small region of the sample is heated by a pulsed CO_2 laser. The heated volume has the form of a flat disk (absorption depth $\cong 30$ μm; beam diameter 4–6 mm) which, by expanding, causes a longitudinal sound pulse. This mechanism of sound excitation by thermal expansion is also utilized by Nelson *et al.* for impulsive stimulated thermal scattering.[1] However, one difference is that there the frequency of sound is tunable from the MHz to the GHz region, whereas here the frequency band is fixed and determined by the duration of the heating pulse and the product of the absorption coefficient and the sound velocity; it falls into the MHz region with an average frequency of $\nu \cong 2$ MHz and falls off to the 20% level at about $\nu \cong 0.2$ MHz and $\nu \cong 5$ MHz. Common to both methods is, while working in the time domain, the possibility to observe, depending on the system under study, delayed thermoelastic responses. For studying glass forming systems, this is a very interesting feature.

The technique which we have just sketched was applied as a first example to a glass-forming room temperature molten salt, viz., $(AlCl_3)_x$ (1-methyl-3-ethyl-imidazoliumchloride)$_{1-x}$, for short called here MEICA. MEICA belongs to a group of metal organic salts which have attracted considerable attention mainly in view of possible applications as liquid electrolytes or solvents which can operate at ambient temperatures.[2] At compositions around the two eutectics, $0.32 \leqslant x \leqslant 0.42$ and $0.61 \leqslant x \leqslant 0.68$, MEICA can be easily supercooled, and at still lower temperatures a glass transition is induced. For the compositions under study in this work, $x=0.36$, $x=0.407$, and $x=0.64$, the reported glass transition temperatures (T_g) are -68 °C, -76 °C, and -95 °C, respectively.[3] The last one is ≈ 60 °C lower than the freezing point.

Quite generally, the mechanical properties of molten salts are of interest in themselves, for applications (especially transport), and as supplementary evidence for questions of structure and bonding. Except for a viscosity measurement,[3] no study of the complex elastic modulus of MEICA seems to exist.

II. EXPERIMENT

A. Optical setup

As the pulsed heat source, a commercial CO_2 laser (Uranit) is used which produces typically 2 J pulses consisting of a narrow [100 ns full width at half maximum (FWHM)] spike, followed by a slow ($\geqslant 1$ μs, 20% amplitude) trailer.

Observation of the propagating sound pulse(s) is performed in a Mach–Zehnder interferometer[4] to which a facility for the measurement of the time evolution has been added. The sample is placed into one of the two interferometer light beams (''sample beam'') so that the light crosses perpendicularly the propagation direction of the sound pulse front at a given distance behind the entrance window for the IR beam (adjustable to 50 μm–50 mm with an accuracy of 1 μm).

The longitudinal acoustic sound pulse produces a change of the optical density (via the molecular density) thus introducing for the sample beam a phase shift with respect to the second, the ''reference beam.'' This shift is measured by the intensity of the interference signal using an avalanche diode driven below its threshold (current mode). For the interferometer we use a commercial He–Ne laser (polarized, 2 mW, beam diameter <1 mm). In order to avoid optical path changes of multiples of the wavelength, we reduce the IR power until the change is less than 0.1λ ($\lambda = 0.633$ μm). The interferometer is set to operate around a phase shift of $\lambda/4$ (mod. λ) when no pulse crosses the sample beam, making its response approximately linear for increase as well as de-

 0021-9606/95/103(22)/9574/6/$6.00

crease of optical path length. To ensure that, it is stabilized at the corresponding level of intensity (50% of full modulation) by shifting piezoelectrically the mirror in the reference beam. The fastest response time of the stabilization was set to stay somewhat below 1 ms, far beyond the sound pulse observation time which is some microseconds. The stabilization serves also to compensate mechanical vibrations of the interferometer.

Two lenses, operating as a telescope, produce in the detector plane an image of the object zone in the sample which is enlarged by a factor of about 60. This avoids distortions of the signal due to diffraction of light by the sound pulses, so that one observes the pulse as a phase-shifting object like in a phase-contrast microscope. The sensitive area of the diode corresponds to a spatial resolution along the sound propagation axis of 10–30 μm.

Characteristic for the method used here is the fact that one integrates the optical density change along the path of the He–Ne laser beam within the sample. It follows that the three-dimensional phase object is projected on a two-dimensional plane, perpendicular to the He–Ne beam.

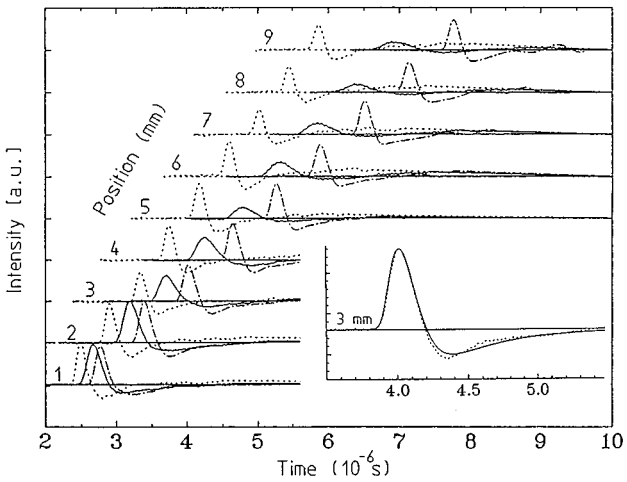

FIG. 1. Sound pulses (MEICA; $x=0.36$) measured at various distances behind the entrance window of the CO_2 beam and at three temperatures: -61 °C (dotted-), -36 °C (full-), and $+15$ °C (dash-dot line). Inset: Comparison of experimental (dotted-) and theoretical (full line) pulse shape. For the parameters used see text.

B. Sample cuvettes and thermostat

The cuvettes are rectangular glass tubes of about 3–5 cm length and an inner base of 1 cm×1 cm (wall thickness 5 mm). One end of such a tube is closed with a high-purity Si window of 0.5 mm thickness, which allows for transmission of CO_2 laser radiation. The other end is closed by a metallic plate, which is glued to the glass or sealed with a teflon ring, and contains a closable access for filling the tube with the liquid under study.

For measurements of temperature dependences, the sample is placed within an evacuated thermostat which also has two plane parallel glass windows (2 cm×10 cm). The CO_2 laser beam penetrates through a Si window into the thermostat. Cooling is done by a flow of liquid alcohol through two copper plates which are pressed against the sample cuvette from above and below. Heating is done by thermocoax wires fixed onto the copper plates. The temperature uncertainty, mainly due to temperature gradients, is ~0.5 °C, and the stability better than 0.1 °C.

C. Sample preparation

Both components, 1-methyl-3-ethyl-imidazolium-chloride (MEIC) and $AlCl_3$ (A) were supplied by Aldrich. The purity of $AlCl_3$ was quoted as 99.99% and for MEIC as 98%. The salt mixtures were prepared in a glove box filled with argon. The crystalline $AlCl_3$ was slowly added to the liquid MEIC to avoid strong temperature increase and chemical decomposition due to the strongly exothermic reaction. Three compositions were prepared having $x=0.36$, 0.407, and 0.64 $AlCl_3$ molefraction, respectively. The sample cuvettes were filled and sealed within the glove box.

D. Measurements and results

To study the traveling LA sound pulse, the sample was shifted perpendicularly to the direction of the sample beam in steps of 1 mm. The interferometer signal was measured with a fast transient digitizer (Hewlett Packard 541a; rate of digitizing: 10 ns). Summing up over 10 shots at every distance was normally enough to get a sufficiently smooth curve. A typical result is displayed in Fig. 1. Three position-dependent measurements on MEICA ($x=0.36$) at three different temperatures are shown. The set in the middle of Fig. 1 is taken at a temperature of strong relaxation and dispersion, which causes pronounced damping and broadening of the pulses. The other two sets belong to lower (left) and higher (right) temperatures, respectively. The difference in sound velocity is clearly reflected by the different time delay.

From each set of spectra (various z-values; fixed T and x) we extracted from the positive part of the sound pulse the position of the maximum, the half width at half maximum, and the pulse height. The pulse positions yield the effective LA sound velocity [see Fig. 2(a)]. The time scatter of the pulse positions was generally below 10 ns, which leads to an uncertainty of less than 2 m/s.

The typical S-bended shape of the LA velocity curve as function of temperature indicates the crossover from the adiabatic sound velocity c_0 to the high frequency value c_∞ (particularly clear for $x=0.36$). In the transition region (-10 to -50 °C for $x=0.36$) the sound velocity change is accompanied by strong relaxation, here expressed in a remarkable increase of the pulse width [see Figs. 3 and 4(b)] and in a decrease of the amplitude [Fig. 4(a)]. From this, we find the maxima of relaxation at -32 °C ($x=0.36$) and at -46 °C ($x=0.407$). The onset of relaxation for $x=0.407$ and $x=0.64$, compared to $x=0.36$, is shifted from -10 °C to lower temperatures by roughly 25 and 50 °C, respectively. The reported[3] glass temperatures T_g shift somewhat less, viz., -8 and -27 °C, respectively.

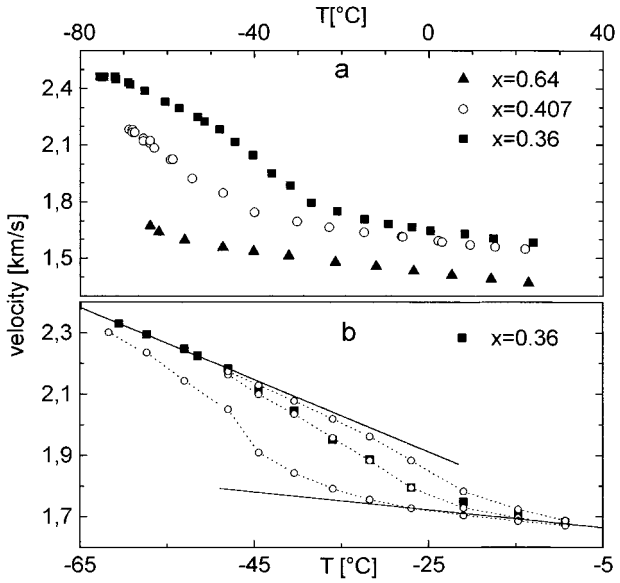

FIG. 2. (a) Sound velocities as taken from the peak of the pulses for three concentrations x. (b) Sound velocities for $x=0.36$ as above and evaluated by simulation (empty circles, dotted lines) with $\nu=0.5$ MHz (lower-), $\nu=2$ MHz (middle-) and $\nu=5$ MHz (upper curve). Straight lines are fits of c_0 (lower) and c_∞ (upper) to experimental data.

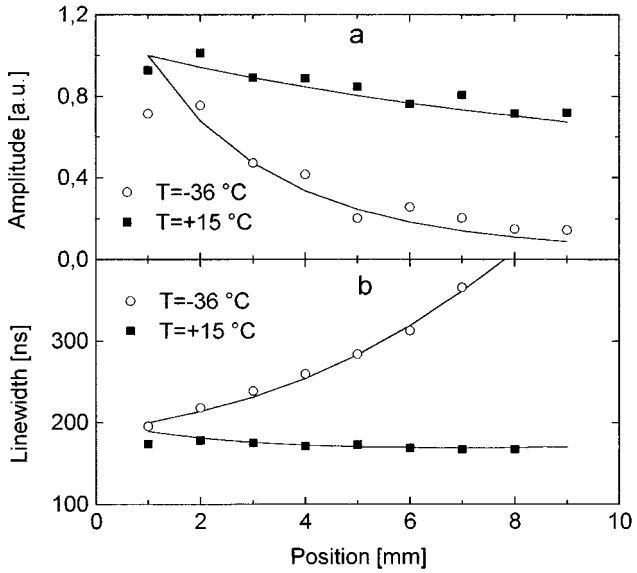

FIG. 4. (a) Experimental (symbols) and simulated (lines) pulse heights for $x=0.36$ at two different temperatures. (b) Same as above, but widths instead of heights.

III. SIMULATION

A. Thermoelastic transfer function

To get a theoretical formulation of the sound pulse, which is produced by radiative heating, we follow a procedure from the literature.[5] Starting from linear hydrodynamics, one derives an inhomogeneous wave equation for the excited excess acoustic pressure. The inhomogeneity derives from the heating by the CO_2 laser pulse. Fourier transformation yields a solution of the traveling pulse at arbitrary distances, excluded is only the heated disk. In the paraxial approximation, the result for the excess pressure $p(t,z)$ at position z (normal distance from the irradiated surface) and at time t reads

$$p(t,z)=\mathrm{real}\left\{B\int_{-\infty}^{\infty}f(\nu)K(\nu)\Phi(\nu)\times\exp\left[i2\pi\nu\left(t-\frac{z}{c_0}\right)\right]d\nu\right\}, \tag{1}$$

where $f(\nu)$ is the frequency spectrum of the heating laser pulse and $K(\nu)$ is the thermo-elastic transfer function. For points near the z axis, the fact that the problem is actually three-dimensional can be taken into account by the diffraction function $\Phi(\nu)$.

The transfer function, taken to be the one for a rigid boundary, since the liquid/glass is in contact with the Si window, and the diffraction function read

$$K(\nu)=\nu_0(1+(\nu/\nu_0)^2)^{-1}; \tag{2a}$$

$$\Phi(\nu)=i\nu(1+iD\nu/\nu_0)^{-1}, \tag{2b}$$

where $\nu_0=\alpha_0 c_0/2\pi$ is the characteristic frequency, depending on the absorption coefficient α_0, and on c_0, the sound velocity, and $D=\alpha_0 a^2/2z$ is the diffraction parameter with a the diameter of the heated disk, i.e., of the CO_2 laser beam.

By inspecting the experimental time dependence of our CO_2 pulse, measured separately with a photon drag detector, we found that its intensity $I(t)$ is reasonably well described by a function assumed in the literature for the same purpose,[6]

$$I(t)=I_0 f(t/\tau_R)=I_0 e^3(t/\tau_R)^3\ \exp\ (-3t/\tau_R) \tag{3}$$

from which we find by Fourier transformation $f(\nu)$. The time, at which the laser pulse reaches its maximum, is $\tau_R=120$ ns. The coefficient B in Eq. (1) equals $B=\pi a^2\beta\alpha_0 I_0/(2C_p z)$ with β the cubic expansion coefficient and C_p the heat capacity of the irradiated medium.

If in Eq. (1) one neglects $\Phi(\nu)$, one sees that $p(t,z)$ depends only on the co-moving coordinate $(t\text{-}z/c_0)$ and that the pulse shape is determined by the convolution of the laser pulse $f(t)$ with the function $\exp(-\nu_0|t|)$ the form of which is

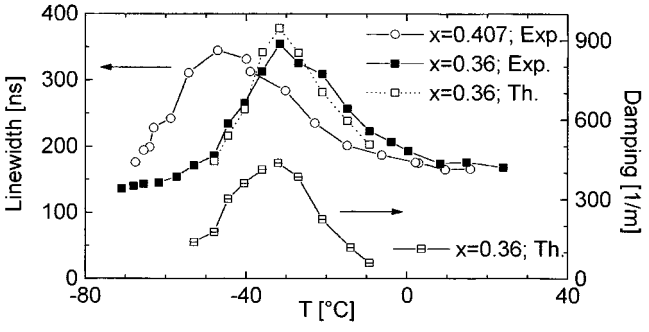

FIG. 3. Experimental line width (FWHM) at $z=6$ mm, for two concentrations x. Included for comparison are linewidth and damping δ from simulation, for $x=0.36$ and $\nu=2$ MHz.

determined by the absorption profile of IR radiation, i.e., $\exp(-\alpha_0 z)$. The consequence of the additional function Φ is to turn the initially unipolar pulse into a bipolar one, with increasing distance z.

The present experiment is sensitive to the density and not to the pressure, and we take one proportional to the other, which is exact for frequency independent c_0 and outside the excitation region.

For the concentration $x=0.36$ we present in the inset of Fig. 1 the experimental pulse shape taken at $T=+14.8$ °C and at $z=3$ mm behind the entrance window, together with the calculated profile using the following set of parameters for the simulation [Eq. (1)]: $\tau_R=140$ ns, $1/\alpha_0=33$ μm, $a=4$ mm and $c_0=1880$ m/s. The calculated amplitude is normalized to match the experimental one. The theory gives the local pressure along the symmetry axis of the sample, but our interferometric technique integrates along the path perpendicular to this direction, i.e., along the curved pulse front, which somewhat increases the observed pulse width. Using $\tau_R=140$ ns instead of $\tau_R=120$ ns (the latter is the proper time constant of the CO_2 pulse), we account for this effect phenomenologically. A good description is achieved. Comparing the sound velocity derived from the peak maxima with the one from simulation, one finds for the latter a value decreased by ~8 m/s with respect to the former. This is mainly due to diffraction of the sound wave, which sharpens the positive part of the pulse while converting the shape from unipolar smoothly into bipolar, as z increases.

B. Damping and dispersion

The classical description of the observed strong damping and dispersion of sound waves in liquids can be traced back to the work of Herzfeld and Litovitz[7] and of Kneser[8] for ultrasonics, and later to that of Zwanzig.[9] They divide the specific heat of the system, C_V, into two parts: The first part $\tilde{C}_V$ counts the translational degrees of freedom (the LA phonons and the diffusional, overdamped TA phonons). A second part C', comprises that part of the degrees of freedom of the system which is not in fast equilibrium with the motions first mentioned, and may be called ''internal degrees of freedom.'' These internal degrees of freedom could be identified in some liquids as the higher optical modes,[10] in glass-forming systems they are rather ''structural'' relaxing motions.

A change of temperature in the translational bath, e.g., when an ''adiabatic'' sound wave induces local deformation, is affecting the temperature in the other bath by exchange of energy, until equilibrium is recovered. The coupling strength between the two baths determines the equilibration time τ, which has a pronounced temperature dependence. This time constant is usually called ''structural relaxation time.'' For a characteristic frequency of the deformation, ω, the effective specific heat may be written as

$$[C_V(\omega)]_{\text{eff}} = C_V - C'(\omega), \tag{4}$$

where $C'(\omega)$ accounts for the internal bath.

When $\omega\tau \ll 1$ holds, both baths are in equilibrium during the process and the fraction of the internal bath which is not contributing is zero $[C'(\omega)=0]$, i.e., the effective specific heat equals the static value C_V. On the other hand, when $\omega\tau \gg 1$, all internal degrees of freedom are decoupled $[C'(\omega)=C']$ and the effective specific heat approaches the value of the translational bath: $(C_V)_{\text{eff}}=C_V-C'=\tilde{C}_V$. We write, analogously, for the specific heat at constant pressure $[C_p(\omega)]_{\text{eff}}=C_p-C'(\omega)$, with the same behavior of the limits.

In order to connect the specific heat with the sound velocity one replaces $c_0^2=\gamma_0(\rho_0\kappa_T)^{-1}$ in Eq. (1) by $c_{\text{eff}}^2=\gamma_{\text{eff}}(\rho_0\kappa_T)^{-1}$, with κ_T the isothermal compressibility, and uses

$$\gamma_{\text{eff}} = \frac{C_p - C'(\omega)}{C_V - C'(\omega)} = 1 + \frac{C_p - C_V}{(C_V)_{\text{eff}}}, \tag{5}$$

the ratio of the effective heat capacities. The low and high frequency values for the velocities become

$$c_0^2 = \frac{C_p}{C_V}\frac{1}{\rho_0\kappa_T} = \frac{\gamma_0}{\rho_0\kappa_T} \tag{6a}$$

and

$$c_\infty^2 = \frac{C_p - C'}{C_V - C'}\frac{1}{\rho_0\kappa_T}. \tag{6b}$$

Useful relations are

$$\frac{c_\infty^2 - c_0^2}{c_0^2} = \frac{C'}{C_p}\frac{C_p - C_V}{C_V - C'} \tag{7a}$$

and

$$C' = C_p \frac{c_\infty^2 - c_0^2}{c_\infty^2\gamma_0 - c_0^2}. \tag{7b}$$

Finally we introduce a simple Debye relaxation for $C'(\omega)$, so that the complex effective velocity reads

$$c_{\text{eff}}^2 = \left(1 + \frac{C_p - C_V}{C_V - \dfrac{i\omega\tau}{1+i\omega\tau}C'} \right) \frac{c_0^2}{\gamma_0} = \frac{1}{\rho_0}(M' + iM''), \tag{8}$$

which, for $(c\delta/\omega)^2 \ll 1$, includes in its real part M' the velocity dispersion $M'=\rho_0 \cdot c^2(\omega)$, while its imaginary part M'' gives the frequency dependent damping $\delta=M''\omega/2\rho_0 c^3(\omega)$.

By applying Eq. (1) and Eq. (8) we are now able to describe the sound pulse propagation in the region of relaxation. This approach is similar to the introduction of effective frequency-dependent complex moduli into the solution of simple hydrodynamic equations.

Using Eq. (8), we have to introduce values for the various parameters. The velocities c_0 and c_∞ are obviously changing with temperature also outside the region of relaxation, and we assume linear temperature dependences for both, c_0 and c_∞. For c_0, this behavior is observed in many other liquids too; for c_∞ it may be discussed in terms of a conversion from glasslike to liquidlike properties while increasing the temperature. The result of least-squares fits to the measured velocities are shown in Fig. 2(b) for the case of $x=0.36$. For the density, used in Eq. (8), we find by extrapolation from measurements at room temperature and above[3] to the range covered in this work: $\rho_0=1.28$ g/cm^3. Furthermore, we set $\gamma_0=1.1$, which is a typical value for liquids, and we

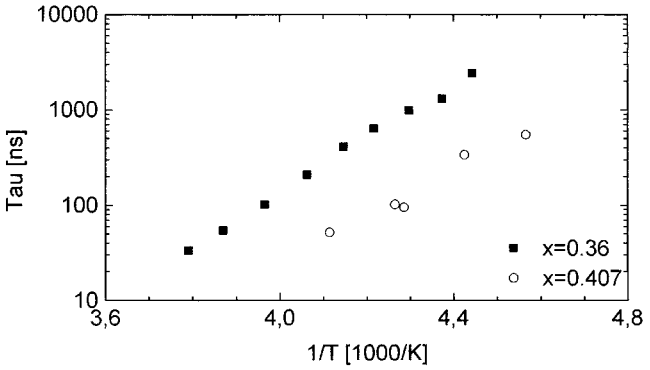

FIG. 5. Relaxation time τ from simulation, for two concentrations x.

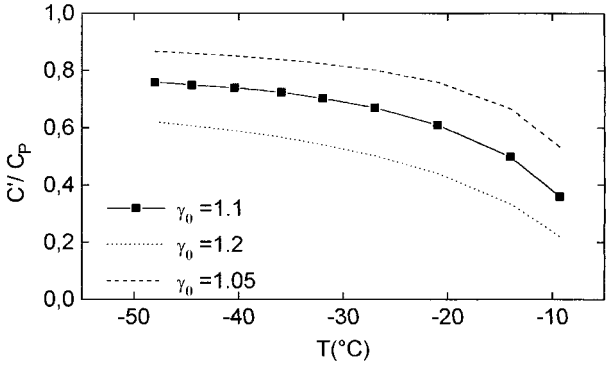

FIG. 6. Normalized heat capacity of the internal bath, $C'(T)$, derived from Eq. (7b) by using different values of γ_0.

normalize all heat capacities by C_p, thus $C_p=1$. Then, from Eq. (7b) we find C', and C_V from Eqs. (6a) and (6b). The only free parameter, i.e., the relaxation time τ, is then determined by simulating the pulse and comparing it to the experimental shape, observed as a function of T through the relaxation region. In order to characterize the shape, we choose the maximum position and its height as well as the FWHM.

Comparison of the simulation with experimental features is made in Figs. 3 and 4(a), 4(b). The overall amplitude factor for the simulation was found by fitting the calculated height to the experimental value at $z=3$ mm. The scatter of the experimental amplitudes is considerable (mainly due to CO_2 laser-power fluctuations), but the general trend is described well by the theory. From the imaginary part of Eq. (8), M'', we calculated the damping δ for the frequency $\nu=\omega/2\pi=2$ MHz and inserted it in Fig. 3. Figure 2(b) gives once more the sound velocity as taken from the delay of the pulse maxima (full squares), but we show additionally the velocity $c(\nu)$ which we computed from the real part of Eq. (8), M', for three representative frequencies ν covering the frequency band of our experiment. The values for the average frequency of 2 MHz coincide well with the values of the group velocities (from peak detection). The spread of the other two curves gives a clear impression of the dispersion.

In Fig. 5 we present $\tau(T)$, one main result from our analysis, for the two concentrations where relaxational phenomena were detectable within our temperature range: $x=0.36$, and $x=0.407$. For the restricted temperature interval where $1/\tau$ crosses the applied range of frequencies, the behavior appears to be Arrheniuslike in both cases. The expected dramatic increase of τ close to T_g is beyond the range where the present experiment is sensitive to τ.

The difference of the high- and the low-frequency sound velocity determines the size of the internal heat bath, the nature of which is of great importance for an understanding of the glass transition. In Fig. 6 we plot the relative magnitude C'/C_p versus temperature [see Eq. (7b)]. It depends on the choice of the value γ_0 as demonstrated by using two other values for it.

IV. DISCUSSION

From x-ray structure analysis[11] it is known that the anionic part of MEICA is established by an equilibrium of $2[AlCl_4]^- \leftrightarrow [Al_2Cl_7]^- + Cl^-$, i.e., single tetrahedra of $[AlCl_4]^-$ and corner-sharing bitetrahedra $[Al_2Cl_7]^-$ plus free Cl^- exist. This is also supported by Raman measurements.[12]

For the cationic part, two models are considered. Fannin *et al.*[13] proposed a model in which the liquid consists of oligomeric chains held together by ion–ion interactions, each MEI cation being associated with two anions; in strong basic liquids these are two chloride ions, one above and one below the plane of the imidazolium ring. The authors exclude explicitly the possibility of hydrogen bonding.

On the other hand, there is evidence from the x-ray crystallographic work of Abdul-Sada *et al.*[14] that the model, proposed by Tait und Osteryoung,[15] is correct. According to it the liquid consists of discrete ion pairs, held together by hydrogen bonds, the anion being Cl^- connected to the cation (imidazolium ring) via a hydrogen bridge to a carbon atom of the distorted imidazolium ring. The position of the anion is not found above the ring, but more in plane.

From this latter model one may expect that the structure of MEICA corresponds to the more fragile systems, in the sense of Angell,[16] which are of a nondirectionally bonded type. The temperature dependence of the correlation time is strongly nonArrhenius for that kind of glass formers, i.e., just above the glass transition temperature the viscosity is expected to drop strongly upon heating. On the other hand, the chain model of Wilkes *et al.* suggests that MEICA tends rather to strong glass formers.

To help to clarify where in Angell's classification scheme MEICA is situated, we plot the shear viscosity revealed from our measurements together with literature values[3] for MEICA as well as for some prominent representatives of fragile and strong glass formers[17] in Fig. 7.

The conversion of our data into low-frequency shear viscosity η_s is done by

$$M_0=K_0=c_0^2\rho_0; \tag{9a}$$

$$M_\infty=K_0+\tfrac{4}{3}G_\infty=c_\infty^2\rho_0; \tag{9b}$$

$$\eta_s=G_\infty\tau=\tfrac{3}{4}(c_\infty^2-c_0^2)\rho_0\tau, \tag{9c}$$

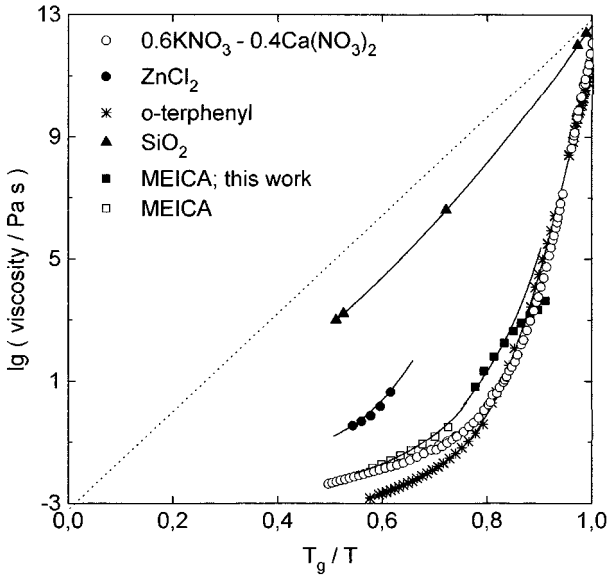

FIG. 7. Viscosities of $0.6KNO_3 0.4Ca(NO_3)_2$ (T_g=333 K), $ZnCl_2$ (365 K), o-terphenyl (240 K), SiO_2 (1453 K) and MEICA (205 K; x=0.36; open squares—literature values, full squares—this work). Lines are guides for the eye.

where we assume that the difference between low (M_0) and high-frequency (M_∞) value of the longitudinal modulus M is solely due to the shear modulus G_∞, because, unfortunately, little is known about the two contributions (bulk and shear) separately. As can be seen from Fig. 7, the two sets of viscosities for MEICA fit well with each other; one is obviously the continuation of the other.

The wrong curvature of our values at the lowest T's reflects the limited validity of our rather simple analysis. We use a single-τ approximation where the behavior of other glass formers suggests rather a broad distribution of τ's. If the latter case holds, our single-τ treatment evaluates a mean τ of only that part of the distribution which overlaps with the time window of the experiment. It would follow for the high-temperature end of the relaxation region that our analysis overestimates the mean τ since a significant portion of the distribution is still below the time window. The corresponding argument leads to an underestimate of τ for the opposite limit of the temperature range. Since in Eq. (9) the approximation for G_∞ is generally accepted (let us say it can at most be wrong by a factor of two) we conclude, in view of Fig. 7, that we missed the real τ by up to one order of magnitude at the lowest temperature.

Nevertheless, Fig. 7 shows clearly that MEICA (x =0.36) tends towards the fragile glass formers and is especially more fragile than $ZnCl_2$, known to have a well-developed network structure. Thus, the ion-pair model of Tait and Osteryoung[15] is favored by our results.

ACKNOWLEDGMENTS

We are obliged to the German-Israeli Foundation for Science and Development (GIF) and to the Deutsche Forschungsgemeinschaft (DFG, Sfb 337) for financial support.

[1] A. R. Douggal and K. A. Nelson, J. Chem. Phys. **94**, 7677 (1991); S. M. Silence, S. R. Goates, and K. A. Nelson, Chem. Phys. **149**, 233 (1990).
[2] For several recent studies see various contributions in: *Proceedings of The Ninth International Symposium on Molten Salts*, edited by C. L. Hussey, D. S. Newman, G. Mamantov, and Y. Ito (Electrochemical Society, Pennington, NJ, 1994).
[3] A. A. Fannin, Jr., D. A. Floreani, L. A. King *et al.*, J. Phys. Chem. **88**, 2614 (1984).
[4] Interferometric techniques have been in use for a long time for the determination of the refractive index, for example: S. E. Gustafson and E. Karawacki, Appl. Opt. **14**, 1105 (1975).
[5] L. V. Burmistrova, A. A. Karabutov, A. I. Portnyagin, O. V. Rudenko, and E. B. Cherepetskaya, Sov. Phys. Acoust. **24**, 369 (1978); A. A. Karabutov, O. V. Rudenko, and E. B. Cherepetskaya, *ibid*. **25**, 218 (1979); **26**, 218 (1980).
[6] M. Tercic and M. W. Sigrist, J. Appl. Phys. **56**, 93 (1984).
[7] K. F. Herzfeld and T. A. Litovitz, *Absorption and Dispersion of Ultrasonic Waves* (Academic, New York, 1959).
[8] H. O. Kneser, Ann. Physik **32**, 277 (1939).
[9] R. Zwanzig, J. Chem. Phys. **43**, 714 (1965).
[10] T. Dorfmüller and D. Samios, Mol. Phys. **41**, 637 (1980); *Fast Reaction in Energetic Systems*, edited by C. Capellos and R. F. Walker (Reidel, Dordrecht, 1981), p. 445.
[11] S. Takahashi, N. Koura, M. Murase, and H. Ohno, J. Chem. Soc. Faraday Trans. 2 **82**, 49 (1986).
[12] B. Gilbert, J.-P. Pauly, Y. Chovin, and F. Di Marco-Van Tiggelen, Ref. 2, pp. 218–226.
[13] A. A. Fannin, Jr., L. A. King, J. A. Levisky, and J. S. Wilkes, J. Phys. Chem. **88**, 2609 (1984).
[14] A. K. Abdul-Sada, A. M. Greenway, P. B. Hitchcock, T. J. Mohamed, K. R. Seddon, and J. A. Zora, J. Chem. Soc. Chem. Commun. **24**, 1753 (1986).
[15] S. Tait and R. A. Osteryoung, Inorg. Chem. **23**, 4352 (1984).
[16] C. A. Angell, *Relaxation in Complex Systems*, edited by K. L. Ngai and G. B. Wright (Office of Naval Research, Washington, DC, 1984).
[17] $0.6KNO_3 0.4Ca(NO_3)_2$: R. Weiler, S. Blaser, and P. B. Macedo, J. Phys. Chem. **73**, 4147 (1969); H. Tweer, N. Laberge, and P. B. Macedo, J. Am. Ceram. Soc. **54**, 121 (1971); G. J. Ganz, *Molten Salt Handbook* (Academic, New York, 1967); o-terphenyl: W. T. Laughlin and D. R. Uhlmann, J. Chem. Phys. **76**, 2317 (1972); M. Cukierman, J. W. Lane, and D. R. Uhlmann, J. Chem. Phys. **59**, 3639 (1973). $ZnCl_2$: J. D. Mackenzie and W. K. Murphy, J. Chem. Phys. **33**, 366 (1960); SiO_2: H. Scholze and K. J. Kreidl, *Glass-Science and Technology*, edited by D. R. Uhlmann and N. J. Kreidl (Academic, New York, 1986), Vol. 3.